Yongqin Lv ORCID iD: 0000-0001-9030-8006

Reversible two enzyme co-immobilization on pH-responsive imprinted monolith for glucose detection

[Jingyi Luo][1, 2 #]

[Liang Ma][3 #]

[Frantisek Svec][2]

[Tianwei Tan][1, 2]

[Yongqin Lv][1, 2 *]

[1][Beijing Key Laboratory of Bioprocess, College of Life Science and Technology, Beijing University of Chemical Technology, Beijing 100029, China]

[2][Beijing Advanced Innovation Center for Soft Matter Science and Engineering, Beijing University of Chemical Technology, Beijing 100029, China]

[3][Clinical Laboratory, China-Japan Friendship Hospital, Beijing 100029, China]

[#] Jingyi Luo and Liang Ma contributed equally to this work.

This article has been accepted for publication and undergone full peer review but has not been through the copyediting, typesetting, pagination and proofreading process, which may lead to differences between this version and the Version of Record. Please cite this article as doi: 10.1002/biot.201900028.

Correspondence: [Prof. Yongqin Lv, College of Life Science and Technology, Beijing University of Chemical Technology, No 15 North Third Ring East Road, 100029 Beijing, China].

E-mail: [lvyq@mail.buct.edu.cn]

Keywords: [ATRP; Two enzyme co-immobilization; Imprinted; Glucose detection; Monolith]

Abbreviations: [**GOx,** glucose oxidase; **POD,** peroxidase; **GMA**, glycidyl methacrylate; **EDMA**, ethylene dimethacrylate; **AIBN**, azobisisobutyronitrile; **DVB**, divinylbenzene; **ABTS**, 2,2'-azinobis(3-ethylbenzothiazoline-6-sulfonic acid ammonium salt); **HRP**, horseradish peroxidase; **BiBB**, 2-bromoisobutyryl bromide; **4-VPBA**, 4-vinylphenylboronic acid; **DMSO**, dimethyl sulfoxide; **DMF**, *N,N'*-dimethyl formamide; **SI-ATRP**, surface-initiated atom transfer radical polymerization; **EDXS**, energy-dispersive X-ray spectroscopy; **RSD**, relative standard deviation]

Abstract

Detection of the glucose concentration is of great significance. Enzymatic assays are the most commonly used techniques, but the current methodologies face long detection time as well as low operational stability and poor repeatability. In this work, a new enzymatic glucose biosensor based on reversible co-immobilization of horseradish peroxidase and glucose oxidase on a pH-responsive imprinted monolith

has been prepared. The poly(4-vinylphenylboronic acid)-grafted imprinted polymer using horseradish peroxidase as a template was formed via surface initiated atom transfer radical polymerization within the pores of brominated poly(glycidyl methacrylate-co-ethylene dimethacrylate) macroporous monolith contained in a 100 μm I.D. capillary column. The two enzymes conjugate was formed via the strong affinity interaction between biotin-labeled glucose oxidase and streptavidin-labeled horseradish peroxidase. The high affinity and selectivity of imprinted monolith toward its template enabled spatially localized co-immobilization of the two enzymes. The modulation of the external pH value enabled reusability of the biosensor simply using stripping of the inactive enzymes at a low pH value and subsequent immobilization of fresh enzymes at a high pH value. Under the optimized conditions, the enzymatic biosensor featured excellent performance in detection of glucose with a linear range of its concentration from 0.11 to 38.85 mmol/L and a limit of detection of 0.03 mmol/L. A relative standard deviation of 3.7% was calculated from determination of twenty glucose samples. This novel enzymatic sensing system was successfully applied for determination of glucose in human serum, and confirmed an enhancement both in selectivity and specificity compared to the more traditionally clinical methods.

Graphical Abstract

Enzymatic assays for detection of the glucose concentration is of great significance, but the current methodologies face long detection time as well as low operational stability and poor repeatability. In this work, a new enzymatic glucose biosensor based on reversible co-immobilization of horseradish peroxidase and glucose oxidase on a pH-responsive imprinted monolith has been prepared, which features fast kinetics of enzymatic catalysis and enables excellent sensing performance as demonstrated with detection of glucose in the human serum. Our concept can also be adapted to other enzymes thus extending the range of useful applications.

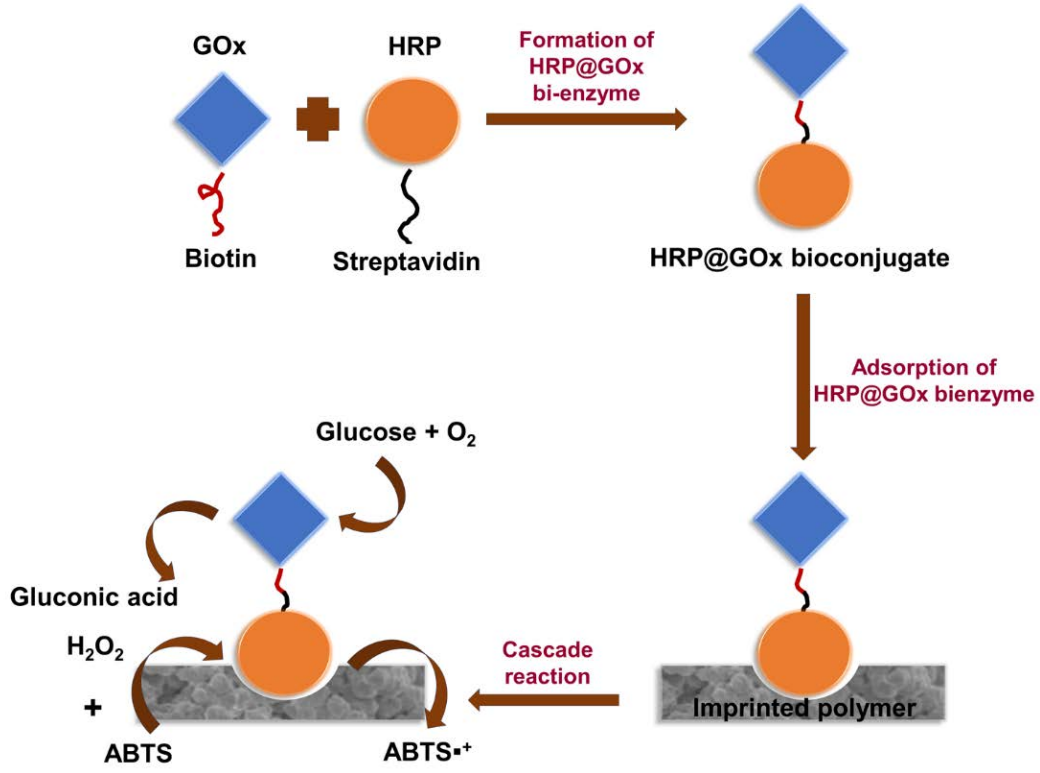

1 Introduction

Glucose circulates in the blood as blood sugar, and is the most important energy reserve and metabolic fuel for cellular respiration [1]. The continuous elevation of blood glucose levels or its deficiency can induce destructive effects on organism functions, such as diabetes and hypoglycemia [2]. Therefore, detection of glucose concentration is of great significance in assisting the diagnosis of diabetes and hypoglycemia as well as monitoring the therapeutic response [3].

A variety of methods have already been developed for the detection and quantification of glucose. These methods can be classified in two categories: (i) enzymatic assays [4] and (ii) non-enzymatic approaches [5-8]. Compared with the latter, enzymatic methods are the most commonly used techniques owing to their high selectivity and specificity, as well as their implementation under mild operational conditions. Enzymatic assays for the detection of glucose involve cascade reactions catalyzed by glucose oxidase (GOx) and peroxidase (POD). In cascade reactions, a reaction intermediate produced from one enzyme is directly utilized by the second enzyme [9]. GOx first oxidizes glucose to gluconic acid and hydrogen peroxide using O_2 as an electron acceptor, and POD then converts H_2O_2 intermediate to H_2O and O_2 [10-12]. However, enzymatic catalysis in solution using free enzymes suffers from several limitations including easy denaturation and deactivation of the enzymes, sample contamination with the enzymes, as well as the difficulties in

enzyme recovery and recycling. In this respect, exploration of solid supports for enzyme immobilization is highly desirable to achieve an increased stability and activity, enhance specificity, avoid contamination with biocatalysts, and facilitate reusability [13-28]. In particular, the co-immobilization of multiple enzymes acting in a cascade reaction is kinetically advantageous [18]. To achieve enhanced activity, the multi-enzyme co-immobilization system should facilitate substrate channeling, kinetics matching, and spatial distribution [29]. The recently reported immobilized enzyme systems for glucose detection are diverse, including magnetic nanoparticles [30, 31], cellulose microspheres [32], graphdiyne [33], carbon nanotubes [34], silicon nanowire arrays [35], metal-organic frameworks [36], hydrogel nanofibers [37], nanoporous gold [38], enzyme-inorganic hybrids [39], enzyme-polymer conjugates [40], and microfluidic device [41, 42]. Although a variety of techniques have been demonstrated enabling co-immobilization of multiple enzymes, several challenges remain such as both enzymes have to be discarded even one of them still has activity and the same immobilization approach may not be optimal for all the enzymes, thus forcing the exploration of new and more general approaches enabling control of the spatial positioning and localization of the enzymes for enhanced stability, activity, and selectivity (or specificity) [43-47].

Porous polymer monoliths which were developed in the early 1990s possess large through pores and high permeability to flow [49-51]. Compared with the porous

particulate supports in which the mass transport of the substrates and products to and from the reaction site is achieved via diffusion through the stagnant liquid phase present in the pores, monoliths enable mass transport to the active site of the enzyme by faster convection rather than by slow diffusion since all the liquid phase must flow through the pores of the support [52]. Moreover, the column format of monolith enables continuous use of the enzyme while no contamination of the products with the biocatalysts occurs. The advantages of monolithic supports for enzyme immobilizations have been demonstrated with several successful examples where immobilized enzymes were used to catalyze substrates dissolved both in aqueous media and organic solvents [52-57]. The drawback of porous polymer monoliths relies on their small surface areas due to the absence of small pores which might result in low immobilization capacities for enzymes. This limitation can be circumvented by grafting a polymer layer on the surface of macropores of monoliths [58-60].

Molecular imprinting technology is a method that is capable of creating a “molecular lock” to match a “molecular key” [61, 62]. This technique leads to synthetic artificial receptors called molecularly imprinted polymers with imprinted cavities complementary to the template molecules in shape, size, and chemical functionality [63, 64]. The current methods also support efficient imprinting of biomacromolecules [65, 66]. We envisaged that use of an enzyme as the template to

construct imprinted cavities would assist oriented immobilization of enzymes and achieve spatial positioning and localization of multiple enzymes. If one enzyme is used as the template to enable the imprinting process, then the generated imprinted cavities would show selective recognition properties towards this enzyme. For multi-enzyme systems, different imprinted cavities produced by different enzymes only have selectivity to their templated enzyme. Thus, by controlling the spatial positioning of imprinted cavities, the localization of multi-enzymes could be controlled.

In this report, we demonstrate the preparation of a new pH-responsive imprinted monolith using surface initiated atom transfer radical polymerization (SI-ATRP) and its use for the oriented reversible immobilization of two enzymes, horseradish peroxidase and glucose oxidase. 4-Vinylphenylboronic acid (VPBA) was selected as the functional monomer to produce the grafted imprinting polymer layer, which can form stable covalent cyclic esters with cis-diol-containing glycoproteins in an alkaline aqueous solution. Boronate esters can be cleaved to release the cis-diol-containing molecules when the pH is changed to acidic. Using this approach, reversible enzyme immobilization can be achieved. The high selectivity and specificity of imprinted polymer for its enzyme template enables spatial positioning and localization of two enzymes, and significantly enhances the biocatalysis efficiency. The pH responsive behaviour permits both selective immobilization and

release of inactive enzymes controlled by just changing the external pH. This property aids repeated use of the support for immobilization of fresh enzymes. We also demonstrate that the monolithic enzyme biosensor enables accurate and sensitive detection of glucose in human serum.

2 Materials and methods

A complete description of chemicals, materials, instrumentation, and preparation of pH-responsive imprinted monoliths is available in the Supporting Information.

2.1 Rebinding of HRP-imprinted monoliths

The typical procedure for enzyme adsorption was as follows: 2 mg/mL HRP solution dissolved in 20 mmol/L phosphate buffer (pH 8.5) was continuously pumped through the imprinted monolith at a flow rate of 0.5 μL/min at 25 ℃ for 1 h to achieve the immobilization. Boronate esters between glycans of HRP and boronic acid groups were formed at pH 8.5. The effluent leaving the capillary outlet was collected for determination of enzyme concentration using HPLC. The adsorption capacity (Q) of imprinted or non-imprinted monoliths was calculated according to Eq. (1):

$$Q = \frac{(C_0 - C)V}{m} \quad (1)$$

where C_0 is the initial concentration of enzyme (mg/mL), C is the final enzyme concentration in the effluent (mg/mL), V is the volume of the solution (mL), and m (mg) is the dry weight of monolith.

The imprinting factor (IF, α) was used to characterize selectivity of the imprinted monoliths (Eq. 2):

$$\alpha = \frac{Q_{MIP}}{Q_{NIP}} \quad (2)$$

where Q_{MIP} and Q_{NIP} are the adsorption capacities of imprinted monolith and non-imprinted monolith for the template enzyme, respectively.

2.2 Enzyme activity

A solution of ABTS with a concentration of 1 mg/mL containing 0.005% H_2O_2 was continuously pumped through the monolithic bioreactors at a flow rate of 0.5 μL/min at 25 °C for 10 h to evaluate the enzyme activities of HRP immobilized on imprinted and non-imprinted monoliths. The effluent leaving the capillary outlet was collected every two hours and the ABTS concentration determined at 405 nm.

2.3 Co-immobilization of HRP and GOx

The HRP@GOx bioconjugate was obtained by mixing 1 mg/mL biotin-labeled glucose oxidase and 1 mg/mL streptavidin-labeled horseradish peroxidase in 20 mmol/L phosphate buffer (pH 8.5) at room temperature for 30 min. It was then

continuously pumped through the imprinted and non-imprinted monoliths in a capillary at a flow rate of 0.5 μL/min at 25 °C for 1 h to achieve the saturation. The monolithic bioreactors were then washed with 20 mmol/L phosphate buffer (pH 8.5) for 0.5 h to remove the non-immobilized enzymes.

Glucose solutions with different concentrations were mixed with 20 mg/mL ABTS at a volume ratio of 1:1 in 20 mol/L phosphate buffer at the optimum pH 7.0 to test the enzyme activity of the immobilized two enzymes. This solution was then continuously pumped through the imprinted or non-imprinted bioreactors at a flow rate of 0.5 μL/min at 25 °C. The effluent was collected and the concentration of $ABTS^{\bullet+}$ product determined at 405 nm using a spectrophotometer.

2.4 Kinetics study

The cascade kinetics study for the two enzyme systems was carried out using glucose and ABTS as substrates. In the presence of oxygen, GOx oxidized glucose to gluconic acid and H_2O_2 intermediate. HRP then catalyzed the oxidation reaction of ABTS with H_2O_2 to $ABTS^{\bullet+}$, which can be recorded at 405 nm. A glucose solution (1 mL) with concentrations ranging from 1 to 100 mmol/L containing 109 mg/mL ABTS in phosphate buffer (pH=7) was continuously pumped through the imprinted or non-imprinted bioreactors at a flow rate of 0.5 μL/min at 25 °C for 30 min. The effluent was collected and analyzed immediately by UV/vis spectrophotometry at

405 nm to determine the concentration of produced $ABTS^{\bullet+}$. The kinetic parameters were calculated from the Lineweaver-Burk plot.

2.5 Glucose detection in human blood

Human blood samples were provided by Clinical Laboratory of China-Japan Friendship Hospital. Prior to analysis, the blood samples were centrifuged at 8000 rpm for 10 min, and the supernatant was collected and mixed with 20 mg/mL ABTS at a volume ratio of 1:1. The serum sample was then continuously pumped through the HRP@GOx immobilized monolith. The effluent was collected, diluted 40-fold, and concentration of the $ABTS^{\bullet+}$ product determined at 405 nm. The amount of glucose was calculated according to the $ABTS^{\bullet+}$ product, and the molar ratio of glucose and $ABTS^{\bullet+}$ was 1:2.

All experiments were carried out in triplicates.

3 Results and discussion

3.1 Preparation of HRP-imprinted monoliths

Surface-initiated atom transfer radical polymerization (SI-ATRP) was used to prepare HRP-imprinted polymer within the pores of a macroporous monolith contained in a 100 μm I.D. capillary. The synthetic approach is illustrated in Scheme 1A. The monolithic support was first synthesized via thermally initiated free-radical

polymerization using GMA as the functional monomer and EDMA as the cross-linker. The epoxide functionalities were modified with ethylenediamine and then reacted with BiBB in a moisture-free environment to introduce the ATRP initiator. Energy-dispersive X-ray spectroscopy (EDXS) revealed 14.1 at% N and 3.8 at% Br in aminated and brominated monoliths, respectively. These values confirmed successful functionalization of the monoliths. Then, the HRP-imprinted polymer layer with tailored binding sites was grafted on the pore surface of monolith via surface-initiated ATRP.

The HRP template and 4-VPBA first self-assembled in a pre-polymerization mixture to form a strong complex via reversible covalent bonds between boronic acid and glycans of HRP. Then the divinylbenzene cross-linker, ATRP ligand (*N*,*N*,*N*′,*N*′,*N*″-pentamethyl diethyenetriamine) and CuBr catalyst were added in the polymerization mixture to initiate the ATRP reaction. We varied two parameters that might affect properties of the imprinted monoliths, i.e. type of catalyst and reaction time, to obtain the optimized support. Both adsorption capacity and selectivity of the imprinted monolith toward HRP template were used to evaluate the effects of these parameters. Figure 1(A, B) confirms that the optimal reaction conditions include the use of CuBr as the catalyst and an ATRP reaction time of 100 min. Using these conditions, the imprinted monolith featured an adsorption capacity of 121.5 mg/g and an imprinting factor of 5.6 for HRP.

3.2 Characterization of HRP-imprinted monoliths

Good permeability is desirable for flow-through applications of monolithic columns. The layer of the ATRP grafted polymers does not fill the pores to produce any significant obstacles to flow through the monoliths as demonstrated with the plots showing back pressure as a function of flow rate for both generic and imprinted monoliths prepared from a polymerization mixture containing 30% cyclohexanol and 30% 1-dodecanol (all wt%) as porogens (Figure S1-A in the supporting information). While the back pressure of generic monolith was only 3.0 MPa/cm capillary column at a flow rate of 5 μL/min using 20 mmol/L phosphate buffer (pH 7) as the mobile phase at room temperature, an increase in the back pressure to 34.3 MPa was observed for its grafted counterpart under the same operational conditions. To further increase the permeability of the grafted monolith, we prepared generic monolith from a polymerization mixture containing 40% monomers, 42% cyclohexanol, and 18% 1-dodecanol. Figure S1-B in the supporting information confirms that the grafted monolith in this case possessed better permeability demonstrated with a decrease in the back pressure to 28.6 MPa at a flow rate of 5 μL/min. The adsorption capacity of this imprinted monolith increased to 240 mg/g with an imprinting factor of 5.7 thanks to the higher permeability of the monolithic structure. Images of the internal morphology of the optimized monolith in dry state before and after grafting copolymerization are shown in Figure 1(C, D).

The generic monolith consists of non-porous interconnected microglobules with large-through pores among the clusters. These microglobules were then covered with the grafted polymer and became larger. This change again confirms the successful formation of imprinted polymer layer.

3.3 Selectivity of HRP-imprinted monoliths

The imprinted and non-imprinted monoliths were further tested for its selectivity against interfering proteins such as cytochrome c and myoglobin. As shown in Figure 1E, the imprinted monolith exhibited an adsorption capacity of 240.24 mg/g for HRP, while the adsorption capacity of non-imprinted monolith towards HRP was mere 42.92 mg/g. The superiority of the imprinted monolith was ascribed to the cavities oriented from the imprinting process. We also found that while the non-imprinted monolith exhibited no selectivity for these proteins, the imprinted monolith featured a good selectivity for its HRP template with an imprinting factor of 5.7. In contrast, the imprinting factors were only 1.66 and 1.33 for the potentially interfering proteins.

The excellent selectivity of the HRP-imprinted monolith was also assessed by testing its enzymatic activity. Both imprinted and non-imprinted monoliths were saturated with HRP and subjected to enzymatic catalysis of reaction of H_2O_2 and ABTS. Horseradish peroxidase catalyzes oxidation of the ABTS substrate to $ABTS^{\bullet+}$

while converting H_2O_2 to H_2O and oxygen. As illustrated in Figure 1F, the amount of $ABTS^{\bullet+}$ produced using the imprinted monolithic biosensor was about 3.5 times larger than that generated from the non-imprinted counterpart. We attribute this remarkable superiority to the ATRP imprinted polymer that provides abundant well-accessible imprinted sites complementary to the HRP template molecule.

3.4 Effects of reaction conditions and pH-responsive property of HRP-imprinted monoliths

Reaction temperature and pH value are important parameters that affect the activity of enzymes. Figure S2 in the supporting information confirms that HRP immobilized on the imprinted monolith had the highest glucose consumption at a temperature of 25 °C and a pH value of 6. Although the optimum pH was 6, the boronate esters needed for enzyme immobilization might be partially cleaved upon acidic condition. Therefore, pH 7 was selected in our further study.

One of the unique properties of our imprinted monolithic biosensor is its pH-response depending on external pH. Reversible enzyme immobilization was attained via the boronate affinity for the targeting HRP glycoprotein, which was formed in solution at an alkaline pH and dissociated at acidic condition. To elucidate this property, the imprinted monolith was first saturated using 2.0 mg/mL HRP solution at pH 8.5. Then the monolith was washed with acetonitrile/water/TFA

(50:49:1, v/v/v) mixture at pH 2 at a flow rate of 0.5 μL /min for 1 h. The adsorption capacity of the imprinted monolith toward HRP was then expressed as the function of pH (Figure 1G). At pH 8.5, the target HRP was captured in the imprinted cavities due to the formation of covalent boronate bonds and the adsorption capacity was 225.3 mg/g. However, the adsorbed HRP was released from the grafted layer at pH 2 owing to the cleavage of the boronate bonds. The adsorption capacity was reduced to 19.1 mg/g. The "smart" pH response of the imprinted monolith enabled the selective capture and easy release of the target enzyme and facilitated regeneration of the catalytic activity of monolithic reactor. We repeated this regeneration for three times reaching a similar activity each time. A relative standard deviation of 5.2% was obtained from three repeated measurements.

The typical reversible immobilization methods are based on the strong physical adsorption between the solid support and enzyme. Using this protocol, the inactive enzyme can be easily released and permit the reuse of the support after the enzyme was stripped away [18]. However, physical adsorption of the enzymes may not be strong enough to avert the loss of the enzyme during the operation. Our new approach involves the use of reversible covalent coupling protocol including the boronic acid containing imprinted monolith as the solid support. The merits of our new approach include: (i) the high permeability of monolithic support provides rapid convective mass transport for substrates and products; (ii) the increase in the

surface area contributed by the grafted polymer layer; (iii) the control of spatial co-localization of enzymes using the imprinted cavities; (iv) the strong covalent bonds preventing leakage of the enzyme during operation; (v) the formation of covalent bonds achieved under very mild conditions; and (vi) facilitation of regeneration of the enzyme activity simply by removing the inactive enzyme at acidic pH, and subsequently immobilizing a fresh enzyme from an alkaline solution.

3.5 Design of HRP@GOx system and its kinetics study

The HRP@GOx two enzyme conjugate was first generated via the strong affinity interaction between biotin-labeled GOx and streptavidin-labeled HRP. The HRP@GOx two enzyme conjugate was then immobilized on the HRP-imprinted monolith through its selective recognition towards HRP (Scheme 1B). The cascade reaction catalyzed by GOx and HRP using glucose and ABTS as substrates includes two steps. First, GOx oxidizes glucose to gluconic acid and H_2O_2 utilizing molecular oxygen as an electron acceptor. Second, HRP converts hydrogen peroxide intermediate to water and oxygen during which the ABTS substrate is transformed to ABTS$^{\bullet+}$. We monitored the biocatalysis kinetics of GOx using glucose substrate at a concentration ranging from 0.25 to 100 mmol/L to assess the performance of the immobilized enzymes in comparison to that of its counterparts in solution. The kinetics curves in Figure 2(A-D) were obtained by plotting glucose concentration versus reaction rate. As expected, the reaction rate got boosted with an increase in

glucose concentration at the initial reaction stage, and then gradually achieved the maximum reaction rate V_{max}. The immobilized enzymes are characterized with a Michaelis constant K_m of 0.6 mmol/L and a maximum reaction rate V_{max} of 15.0 μmol/L.min in comparison to a K_m value of 2.5 mmol/L and a V_{max} value of 7.6 μmol/L.min for free enzymes in solution. A low K_m value indicates a high affinity between the enzyme and substrate. In usual cases, the immobilized enzymes exhibit a higher K_m than free enzymes due to the steric hindrance and partial inactivation of enzymes during the immobilization process [12, 67]. In contrast, the apparent K_m value of immobilized enzyme in our study was remarkably decreased as compared with that of the soluble counterpart. This increased affinity between immobilized enzyme and substrate indicates that the use of imprinted monolith as the solid carrier could decrease the substrate inhibition of enzyme [68]. A reduction in the K_m value was also found in other studies [12, 67, 69-71]. The V_{max} value of immobilized enzyme is almost twice of that observed for the soluble enzyme indicating a faster reaction rate. Our results clearly demonstrate the superiority of immobilized enzymes derived from the selectivity of imprinted polymer layer and high permeability of monolithic solid support.

3.6 Reproducibility, repeatability, stability, and reusability

The reproducibility and repeatability of glucose sensor was determined using a substrate solution containing 5.55 mmol/L glucose and 36.45 mmol/L ABTS. The

relative standard deviation (RSD) based on five independently prepared monolithic biosensors was 4.3%, indicating a good reproducibility. The repeatability of the glucose sensor was evaluated by twenty successive enzymatic measurements of the glucose solution. A RSD of 3.7% was found demonstrating the excellent repeatability.

The operational stability of enzymatic glucose sensor is another important parameter that affects the real-life applications. We tested the operational stability by continuously pumping the glucose substrate through the reactor and determining the yield of gluconic acid. Figure 2E demonstrates that no noticeable decrease in glucose conversion occurred until 1791 reactor volumes were converted. After this point, glucose conversion decreased dramatically presumably as a result of the leakage or deactivation of the enzymes. The pH-responsive property of our imprinted monolithic device facilitates regeneration of the activity of the biosensor simply by removing the inactive enzymes using buffer with acidic pH, followed by recharging of the biosensor with the fresh enzymes. The amount of stripped inactive enzymes was measured and calculated. We found that this quantity was similar to that of the freshly immobilized enzyme demonstrating no enzyme leakage after the glucose measurement due to the formation of strong covalent bonds. The regeneration was repeated several times and we obtained the same activity each time. Compared with the conventional disposable GOx-POD test, which can only be used once, our enzymatic glucose sensor appears to be more economically viable.

Also, we did not observe any decrease in the enzyme activity after storing the glucose sensor in refrigerator for three months.

3.8 Application of HRP-imprinted monolith for detection of glucose in human serum

To elucidate the feasibility of glucose sensor in practical application, glucose analysis was performed in pre-treated human serum samples from thirty individuals using our monolithic biosensor. Each serum sample was mixed with equivalent volume of ABTS at a concentration of 20 mg/mL, and pumped through the 3.2 cm long imprinted monolith biosensor containing the immobilized GOx-HRP bioconjugate at 25 °C at a flow rate of 0.5 μL/min. This flow rate corresponds to a residence time of 18 s of the glucose substrates in the reactor. The effluent was collected, diluted 40-fold, and the content of $ABTS^{\bullet+}$ product determined using spectrophotometer at 405 nm. Table S1 in the Supporting Information confirms that the concentration of glucose tested using our monolithic sensor was in a good agreement with the values determined in the hospital using their routine GOx-POD lab method that requires 30 min to complete the measurement. This table demonstrates that our sensor could be a good substitute available for routine analyses of glucose in real biological samples.

The reusability of prepared biosensor in detecting glucose concentration in real blood samples was also studied by measuring fifteen identical samples. As shown in Figure 2F, the biosensor could be reused for twelve times with a relative standard deviation (RSD) of only 1.8%. After measurement of twelve samples, the activity of the immobilized enzymes begun to decrease leaving part of glucose unconverted. Taking advantage of reversible covalent immobilization, the biosensor was regenerated by stripping the inactive enzymes at pH 2 and subsequent immobilizing fresh enzymes at pH 8.5. The regenerated biosensor exhibited the original enzyme activity and stability with a RSD of 1.0% for the measurement of fifteen identical real blood samples. We also evaluated the adsorption capacity of imprinted monolith towards blood samples, and found that the total protein concentration of blood samples before and after pumping through the imprinted monolith was identical confirming that no interfering proteins were adsorbed.

4 Concluding remarks

We present the preparation of pH-responsive imprinted monoliths and their successful application as solid supports for reversible immobilization of HRP and GOx. Compared with conventional enzyme immobilization approaches, the use of pH-responsive imprinted monoliths provides several advantages including the high specificity and selectivity. Our imprinted monolith enables a controlled spatial positioning and localization of the two enzymes, which facilitates substrate mass

transport and improves efficiency of enzymatic catalysis. The pH-response enables reversible immobilization of enzymes and the repeated application of the monolithic support that remains placed in the reactor all the time. The regeneration of activity of our monolithic biosensor is easily achieved by removing the inactive enzyme at a low pH followed by immobilization of the fresh enzymes at a high pH. This regeneration can have a significant economic effect while applying our device for routine testing of large series of samples. Our monolithic biosensor features fast kinetics of enzymatic catalysis and enables excellent sensing performance as demonstrated with detection of glucose in the human serum. Our concept can also be adapted to other enzymes thus extending the range of useful applications.

Acknowledgement

The authors gratefully acknowledge the financial supports from the National Key Research and Development Program of China (2017YFF0205401), National Natural Science Foundation of China (21576017, 31961133004, 21436002), and the Higher Education and High-Quality and World-Class Universities (PY201613).

Conflict of interest

The authors declare no financial or commercial conflict of interest.

5 References

[1] Galant, A. L., Kaufman, R. C., Wilson, J. D., Glucose: Detection and analysis. *Food Chem.* 2015, *188*, 149-160.

[2] Hwang, D.-W., Lee, S., Seo, M., Chung, T. D., Recent advances in electrochemical non-enzymatic glucose sensors – A review. *Anal. Chim. Acta* 2018, *1033*, 1-34.

[3] van Enter, B. J., von Hauff, E., Challenges and perspectives in continuous glucose monitoring. *Chem. Commun.* 2018, *54*, 5032-5045.

[4] Lv, P., Zhou, H., Mensah, A., Feng, Q., Wang, D., Hu, X., Cai, Y., Amerigo Lucia, L., Li, D., Wei, Q., A highly flexible self-powered biosensor for glucose detection by epitaxial deposition of gold nanoparticles on conductive bacterial cellulose. *Chem. Eng. J.* 2018, *351*, 177-188.

[5] Zhang, Y., Jia, W., Cui, M., Dong, C., Shuang, S., Kwan, Y., Choi, M. M. F., Glucose biosensor based on nanohybrid material of gold nanoparticles and glucose oxidase on a bioplatform. *Biotechnol. J.* 2011, *6*, 492-500.

[6] Qi, L., Hu, Q., Kang, Q., Yu, L., Fabrication of liquid-crystal-based optical sensing platform for detection of hydrogen peroxide and blood glucose. *Anal. Chem.* 2018, *90*, 11607-11613.

[7] Li, A., Mu, X., Li, T., Wen, H., Li, W., Li, Y., Wang, B., Formation of porous Cu hydroxy double salt nanoflowers derived from metal–organic frameworks with efficient peroxidase-like activity for label-free detection of glucose. *Nanoscale* 2018, *10*, 11948-11954.

[8] Xuan, X., Yoon, H. S., Park, J. Y., A wearable electrochemical glucose sensor based on simple and low-cost fabrication supported micro-patterned reduced graphene oxide nanocomposite electrode on flexible substrate. *Biosens. Bioelectron.* 2018, *109*, 75-82.

[9] Walsh, C. T., Moore, B. S., Enzymatic cascade reactions in biosynthesis. *Angew. Chem. Int. Ed.*, *10.1002/anie.201807844*.

[10] Wang, Z., Wang, J., Chen, G., Xu, W., Fu, Z., Jiang, G., Wu, J., Liu, Z., Polyelectrolytes tailored enzyme cascades with enhanced stability and activity for one-pot synthesis. *ChemCatChem* 2018, *10*, 5391-5396.

[11] Wang, Z., Xu, W., Fu, Z., Jiang, G., Wu, J., Liu, Z., Pluronic-conjugated enzyme cascade for in situ oxidation in biphasic media. *ChemCatChem* 2018, *10*, 2003-2008.

[12] Zhang, Y., Yong, Y., Ge, J., Liu, Z., Lectin agglutinated multienzyme catalyst with enhanced substrate affinity and activity. *ACS Catal.* 2016, *6*, 3789-3795.

[13] Bernal, C., Rodríguez, K., Martínez, R., Integrating enzyme immobilization and protein engineering: An alternative path for the development of novel and improved industrial biocatalysts. *Biotechnol. Adv.* 2018, *36*, 1470-1480.

[14] Rodrigues, R. C., Ortiz, C., Berenguer-Murcia, Á., Torres, R., Fernández-Lafuente, R., Modifying enzyme activity and selectivity by immobilization. *Chem. Soc. Rev.* 2013, *42*, 6290-6307.

[15] Hanefeld, U., Gardossi, L., Magner, E., Understanding enzyme immobilisation. *Chem. Soc. Rev.* 2009, *38*, 453-468.

[16] Secundo, F., Conformational changes of enzymes upon immobilisation. *Chem. Soc. Rev.* 2013, *42*, 6250-6261.

[17] Sheldon, R. A., van Pelt, S., Enzyme immobilisation in biocatalysis: why, what and how. *Chem. Soc. Rev.* 2013, *42*, 6223-6235.

[18] Garcia-Galan, C., Berenguer-Murcia, Á., Fernandez-Lafuente, R., Rodrigues, R. C., Potential of different enzyme immobilization strategies to improve enzyme performance. *Adv. Synth. Catal.* 2011, *353*, 2885-2904.

[19] Virgen-Ortíz, J. J., dos Santos, J. C. S., Berenguer-Murcia, Á., Barbosa, O., Rodrigues, R. C., Fernandez-Lafuente, R., Polyethylenimine: a very useful ionic

polymer in the design of immobilized enzyme biocatalysts. *J. Mater. Chem. B.* 2017, *5*, 7461-7490.

[20] Cipolatti, E. P., Valério, A., Henriques, R. O., Moritz, D. E., Ninow, J. L., Freire, D. M. G., Manoel, E. A., Fernandez-Lafuente, R., de Oliveira, D., Nanomaterials for biocatalyst immobilization – state of the art and future trends. *RSC Adv.* 2016, *6*, 104675-104692.

[21] Poppe, J. K., Fernandez-Lafuente, R., Rodrigues, R. C., Ayub, M. A. Z., Enzymatic reactors for biodiesel synthesis: Present status and future prospects. *Biotechnol. Adv.* 2015, *33*, 511-525.

[22] Arana-Peña, S., Mendez-Sanchez, C., Rios, N. S., Ortiz, C., Gonçalves, L. R. B., Fernandez-Lafuente, R., New applications of glyoxyl-octyl agarose in lipases co-immobilization: Strategies to reuse the most stable lipase. *Int. J. Biol. Macromol.* 2019, *131*, 989-997.

[23] Adamíková, J., Antošová, M., Polakovič, M., A method of early phase selection of carrier for Aspergillus Oryzae β-galactosidase immobilization for galactooligosaccharides production. *Biotechnol. J.* 2019, *14*, 1800120.

[24] Barth, M., Honak, A., Oeser, T., Wei, R., Belisário-Ferrari, M. R., Then, J., Schmidt, J., Zimmermann, W., A dual enzyme system composed of a polyester

hydrolase and a carboxylesterase enhances the biocatalytic degradation of polyethylene terephthalate films. *Biotechnol. J.* 2016, *11*, 1082-1087.

[25] Hyeon, J. E., Shin, S. K., Han, S. O., Design of nanoscale enzyme complexes based on various scaffolding materials for biomass conversion and immobilization. *Biotechnol. J.* 2016, *11*, 1386-1396.

[26] Lotti, M., Pleiss, J., Valero, F., Ferrer, P., Enzymatic production of biodiesel: strategies to overcome methanol inactivation. *Biotechnol. J.* 2018, *13*, 1700155.

[27] Bolivar, J. M., Valikhani, D., Nidetzky, B., Demystifying the flow: biocatalytic reaction intensification in microstructured enzyme reactors. *Biotechnol. J.* 2019, *14*, 1800244.

[28] Kamiya, N., Ohama, Y., Minamihata, K., Wakabayashi, R., Goto, M., Liquid marbles as an easy-to-handle compartment for cell-free synthesis and in situ immobilization of recombinant proteins. *Biotechnol. J.* 2018, *13*, 1800085.

[29] Zhang, Y., Ge, J., Liu, Z., Enhanced activity of immobilized or chemically modified enzymes. *ACS Catal.* 2015, *5*, 4503-4513.

[30] Wu, Q., Wang, X., Liao, C., Wei, Q., Wang, Q., Microgel coating of magnetic nanoparticles via bienzyme-mediated free-radical polymerization for colorimetric detection of glucose. *Nanoscale* 2015, *7*, 16578-16582.

[31] Lawson, B. P., Golikova, E., Sulman, A. M., Stein, B. D., Morgan, D. G., Lakina, N. V., Karpenkov, A. Y., Sulman, E. M., Matveeva, V. G., Bronstein, L. M., Insights into sustainable glucose oxidation using magnetically recoverable biocatalysts. *ACS Sustain. Chem. Eng.* 2018, *6*, 9845-9853.

[32] Li, W., Zhang, L., Li, Q., Wang, S., Luo, X., Deng, H., Liu, S., Porous structured cellulose microsphere acts as biosensor for glucose detection with "signal-and-color" output. *Carbohydr. Polym.* 2019, *205*, 295-301.

[33] Liu, J., Shen, X., Baimanov, D., Wang, L., Xiao, Y., Liu, H., Li, Y., Gao, X., Zhao, Y., Chen, C., Immobilized ferrous ion and glucose oxidase on graphdiyne and its application on one-step glucose detection. *ACS Appl. Mater. Inter.* 2019, *11*, 2647-2654.

[34] Rust, I. M., Goran, J. M., Stevenson, K. J., Amperometric detection of aqueous silver ions by inhibition of glucose oxidase immobilized on nitrogen-doped carbon nanotube electrodes. *Anal. Chem.* 2015, *87*, 7250-7257.

[35] Xu, C., Song, Z., Xiang, Q., Jin, J., Feng, X., A high performance three-phase enzyme electrode based on superhydrophobic mesoporous silicon nanowire arrays for glucose detection. *Nanoscale* 2016, *8*, 7391-7395.

[36] Liu, X., Qi, W., Wang, Y., Lin, D., Yang, X., Su, R., He, Z., Rational design of mimic multienzyme systems in hierarchically porous biomimetic metal–organic frameworks. *ACS Appl. Mater. Inter.* 2018, *10*, 33407-33415.

[37] Liang, H., Jiang, S., Yuan, Q., Li, G., Wang, F., Zhang, Z., Liu, J., Co-immobilization of multiple enzymes by metal coordinated nucleotide hydrogel nanofibers: improved stability and an enzyme cascade for glucose detection. *Nanoscale* 2016, *8*, 6071-6078.

[38] Wu, C., Sun, H., Li, Y., Liu, X., Du, X., Wang, X., Xu, P., Biosensor based on glucose oxidase-nanoporous gold co-catalysis for glucose detection. *Biosens. Bioelectron.* 2015, *66*, 350-355.

[39] Li, W., Lu, S., Bao, S., Shi, Z., Lu, Z., Li, C., Yu, L., Efficient in situ growth of enzyme-inorganic hybrids on paper strips for the visual detection of glucose. *Biosens. Bioelectron.* 2018, *99*, 603-611.

[40] Ji, J., Joh, H.-I., Chung, Y., Kwon, Y., Glucose oxidase and polyacrylic acid based water swellable enzyme–polymer conjugates for promoting glucose detection. *Nanoscale* 2017, *9*, 15998-16004.

[41] Agustini, D., Bergamini, M. F., Marcolino-Junior, L. H., Tear glucose detection combining microfluidic thread based device, amperometric biosensor and microflow injection analysis. *Biosens. Bioelectron.* 2017, *98*, 161-167.

[42] Piao, Y., Han, D. J., Azad, M. R., Park, M., Seo, T. S., Enzyme incorporated microfluidic device for in-situ glucose detection in water-in-air microdroplets. *Biosens. Bioelectron.* 2015, *65*, 220-225.

[43] Lin, J.-L., Palomec, L., Wheeldon, I., Design and analysis of enhanced catalysis in scaffolded multienzyme cascade reactions. *ACS Catal.* 2014, *4*, 505-511.

[44] Bugada, L. F., Smith, M. R., Wen, F., Engineering spatially organized multienzyme assemblies for complex chemical transformation. *ACS Catal.* 2018, *8*, 7898-7906.

[45] Sperl, J. M., Sieber, V., Multienzyme cascade reactions-status and recent advances. *ACS Catal.* 2018, *8*, 2385-2396.

[46] Klermund, L., Poschenrieder, S. T., Castiglione, K., Biocatalysis in polymersomes: improving multienzyme cascades with incompatible reaction steps by compartmentalization. *ACS Catal.* 2017, *7*, 3900-3904.

[47] Wahl, C., Hirtz, D., Elling, L., Multiplexed capillary electrophoresis as analytical tool for fast optimization of multi-enzyme cascade reactions-synthesis of nucleotide sugars. *Biotechnol. J.* 2016, *11*, 1298-1308.

[48] Peirce, S., Virgen-Ortíz, J. J., Tacias-Pascacio, V. G., Rueda, N., Bartolome-Cabrero, R., Fernandez-Lopez, L., Russo, M. E., Marzocchella, A., Fernandez-Lafuente, R., Development of simple protocols to solve the problems of enzyme coimmobilization. Application to coimmobilize a lipase and a β-galactosidase. *RSC Adv.* 2016, *6*, 61707-61715.

[49] Svec, F., Lv, Y., Advances and recent trends in the field of monolithic columns for chromatography. *Anal. Chem.* 2015, *87*, 250-273.

[50] Lv, Y., Cao, Y., Svec, F., Tan, T., Porous polymer-based monolithic layers enabling pH triggered switching between superhydrophobic and superhydrophilic properties. *Chem. Commun.* 2014, *50*, 13809-13812.

[51] Lv, Y., Lin, Z., Svec, F., Hypercrosslinked large surface area porous polymer monoliths for hydrophilic interaction liquid chromatography of small molecules featuring zwitterionic functionalities attached to gold nanoparticles held in layered structure. *Anal. Chem.* 2012, *84*, 8457-8460.

[52] Lv, Y., Lin, Z., Tan, T., Svec, F., Preparation of reusable bioreactors using reversible immobilization of enzyme on monolithic porous polymer support with attached gold nanoparticles. *Biotechnol. Bioeng.* 2014, *111*, 50-58.

[53] Wen, L., Gao, A., Cao, Y., Svec, F., Tan, T., Lv, Y., Layer-by-layer assembly of metal–organic frameworks in macroporous polymer monolith and their use for enzyme immobilization. *Macromol. Rapid Commun.* 2016, *37*, 551-557.

[54] Pirozzi, D., Abagnale, M., Minieri, L., Pernice, P., Aronne, A., In-situ sol-gel modification strategies to develop a monolith continuous microreactor for enzymatic green reactions. *Chem. Eng. J.* 2016, *306*, 1010-1016.

[55] Yesil-Celiktas, O., Cumana, S., Smirnova, I., Silica-based monoliths for enzyme catalyzed reactions in microfluidic systems with an emphasis on glucose 6-phosphate dehydrogenase and cellulase. *Chem. Eng. J.* 2013, *234*, 166-172.

[56] Urban, J., Svec, F., Fréchet, J. M. J., A monolithic lipase reactor for biodiesel production by transesterification of triacylglycerides into fatty acid methyl esters. *Biotechnol. Bioeng.* 2012, *109*, 371-380.

[57] Chen P. P., Gong L. J., Lv Y. Q., New development and application of porous monoliths as solid supports for immobilization of enzymes. *Chin. J. Bioproc. Eng.* 2019, *17*, 36-43.

[58] Wen, L., Tan, X., Sun, Q., Svec, F., Lv, Y., "Smart" molecularly imprinted monoliths for the selective capture and easy release of proteins. *J. Sep. Sci.* 2016, *39*, 3267-3273.

[59] Wang, H.-S., Feng, X.-Y., Wei, J.-P., Biocompatible chiral monolithic stationary phase synthesized via atom transfer radical polymerization for high performance liquid chromatographic analysis. *J. Chromatogr. A* 2015, *1409*, 132-137.

[60] Li, N., Zheng, W., Shen, Y., Qi, L., Li, Y., Qiao, J., Wang, F., Chen, Y., Preparation of a novel polymer monolith with functional polymer brushes by two-step atom-transfer radical polymerization for trypsin immobilization. *J. Sep. Sci.* 2014, *37*, 3411-3417.

[61] Chen, L., Wang, X., Lu, W., Wu, X., Li, J., Molecular imprinting: perspectives and applications. *Chem. Soc. Rev.* 2016, *45*, 2137-2211.

[62] BelBruno, J. J., Molecularly imprinted polymers. *Chem. Rev.* 2019, *119*, 94-119.

[63] Pan, J., Chen, W., Ma, Y., Pan, G., Molecularly imprinted polymers as receptor mimics for selective cell recognition. *Chem. Soc. Rev.* 2018, *47*, 5574-5587.

[64] Lv, Y., Tan, T., Svec, F., Molecular imprinting of proteins in polymers attached to the surface of nanomaterials for selective recognition of biomacromolecules. *Biotechnol. Adv.* 2013, *31*, 1172-1186.

[65] Mori, K., Hirase, M., Morishige, T., Takano, E., Sunayama, H., Kitayama, Y., Inubushi, S., Sasaki, R., Yashiro, M., Takeuchi, T., A pretreatment-free, polymer-based platform prepared by molecular imprinting and post-imprinting modifications for sensing intact exosomes. *Angew. Chem. Int. Ed.* 2019, *58*, 1612-1615.

[66] Motib, A., Guerreiro, A., Al-Bayati, F., Piletska, E., Manzoor, I., Shafeeq, S., Kadam, A., Kuipers, O., Hiller, L., Cowen, T., Piletsky, S., Andrew, P. W., Yesilkaya, H., Modulation of quorum sensing in a gram-positive pathogen by linear molecularly imprinted polymers with anti-infective properties. *Angew. Chem. Int. Ed.* 2017, *56*, 16555-16558.

[67] Yuan, B., Yang, X.-Q., Xue, L.-W., Feng, Y.-N., Jiang, J.-H., A novel recycling system for nano-magnetic molecular imprinting immobilised cellulases: Synergistic recovery of anthocyanin from fruit and vegetable waste. *Bioresour. Technol.* 2016, *222*, 14-23.

[68] Busto, M. D., Ortega, N., Perez-Mateos, M., Studies of microbial β-d-glucosidase immobilized in alginate gel beads. *Process Biochem.* 1995, *30*, 421-426.

[69] Gao, Y., Roberts, C. C., Zhu, J., Lin, J.-L., Chang, C.-E. A., Wheeldon, I., Tuning enzyme kinetics through designed intermolecular interactions far from the active site. *ACS Catal.* 2015, *5*, 2149-2153.

[70] Lyu, F., Zhang, Y., Zare, R. N., Ge, J., Liu, Z., One-pot synthesis of protein-embedded metal–organic frameworks with enhanced biological activities. *Nano Lett.* 2014, *14*, 5761-5765.

[71] Yong, Y., Su, R., Liu, X., Xu, W., Zhang, Y., Wang, R., Ouyang, P., Wu, J., Ge, J., Liu, Z., Lectin corona enhances enzymatic catalysis on the surface of magnetic nanoparticles. *Biochem. Eng. J.* 2018, *129*, 26-32.

Figures

Scheme 1. (A) Synthetic approach to the surface modifications of poly(glycidyl methacrylate-co-ethylene dimethacrylate) monolith with ethylenediamine, 2-bromoisobutyryl bromide, followed by surface grafting of HRP imprinted poly(4-VPBA) layer. (B) Schematic illustrations of the positional assembly and spatial co-localization of GOx and HRP on imprinted monolith, as well as the cascade biocatalysis reaction.

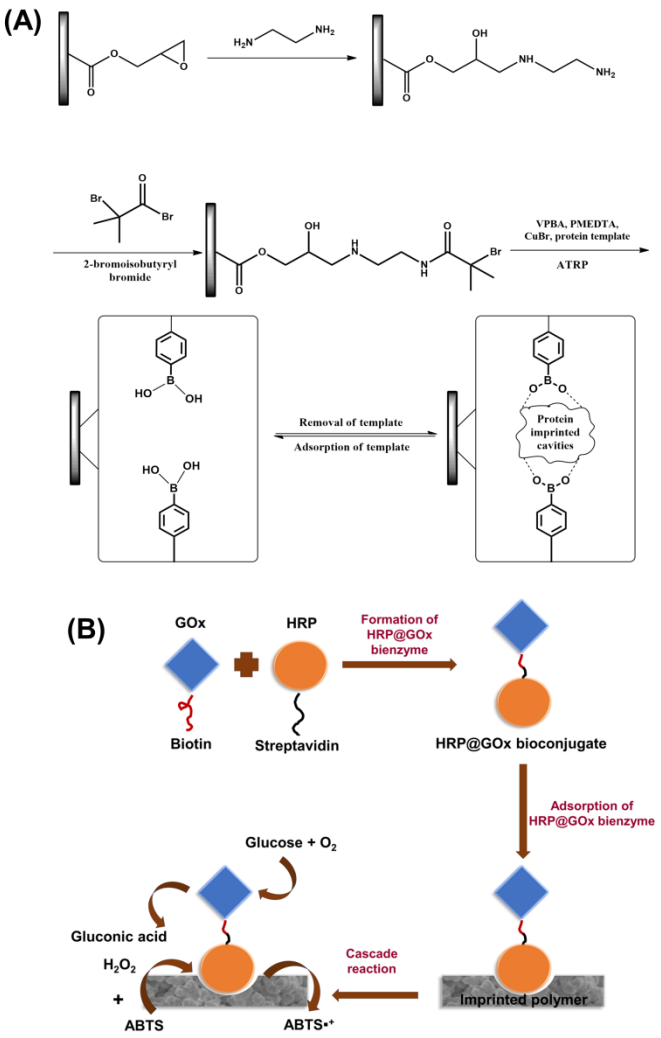

Figure 1. The adsorption capacity (bars) and imprinting factor (lines) of monolith imprinted with horseradish peroxidase (MIP) and non-imprinted monolith (NIP) as the function of ATRP catalyst (A) and ATRP reaction time (B). SEM images of generic monolith (C) and HRP-imprinted monolith (D). The adsorption capacity of the HRP-imprinted and non-imprinted monoliths determined for horseradish peroxidase, myoglobin, and cytochrome C (E). Plots of amounts of ABTS$^{\bullet+}$ product of reaction catalyzed by imprinted and non-imprinted monolithic HRP bioreactor as a function of time (F). The HRP adsorption capacity of imprinted monolith as a function of pH (G).

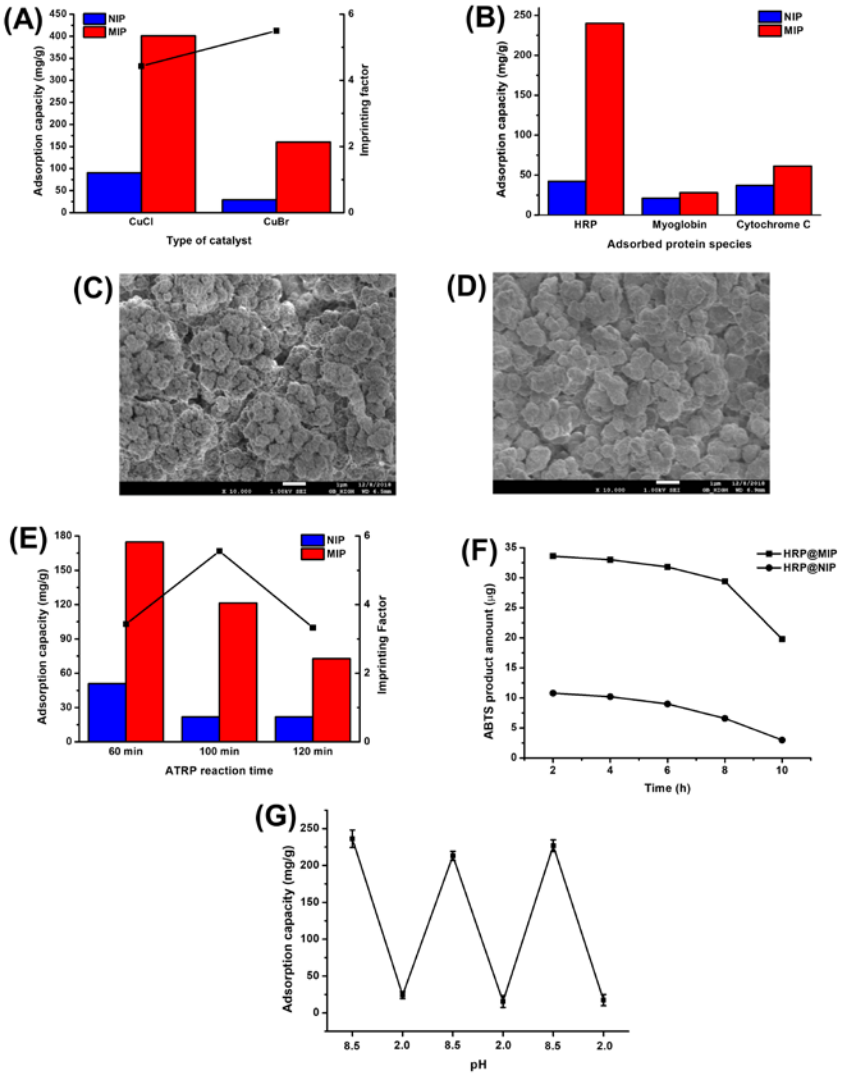

Figure 2. Kinetic plots related to the oxidation of glucose catalyzed using a mixture of GOx and HRP enzymes in solution (A, B), and GOx and HRP immobilized on the functionalized monolith (C, D) (Conditions: pH 7, reaction temperature 25 °C). Change in activity of the immobilized GOx/HRP bioreactor expressed as the yield of gluconic acid with respect to the overall volume of glucose substrate pumped through the monolithic bioreactor (E) (The arrow shows a point at which the activity was restored after stripping the inactive enzymes and immobilizing the fresh ones). Glucose content in plasma of fifteen identical real blood samples measured using our GOx-HRP@imprinted monolithic bioreactor and its regenerated counterpart (F).